

Article

Nitrogen and Phosphorus Removal Efficiency and Denitrification Kinetics of Different Substrates in Constructed Wetland

Yinjin Zeng¹, Weibin Xu^{1,*}, Han Wang², Dan Zhao^{2,*} and Hui Ding²¹ Huadong Engineering (Fujian) Corporation, Fuzhou 350001, China; zeng_yj@hdec.com² School of Environmental Science and Engineering, Tianjin University, Tianjin 300072, China; wanghanleng@126.com (H.W.); dinghui@tju.edu.cn (H.D.)

* Correspondence: xu_wb@hdec.com (W.X.); zhaodan20210430@163.com (D.Z.)

Abstract: Constructed wetlands (CWs) are generally used for wastewater treatment and removing nitrogen and phosphorus. However, the treatment efficiency of CWs is limited due to the poor performance of various substrates. To find appropriate substrates of CWs for micro-polluted water treatment, zeolite, quartz sand, bio-ceramsite, porous filter, and palygorskite self-assembled composite material (PSM) were used as filtering media to treat slightly polluted water with the aid of autotrophic denitrifying bacteria. PSM exhibited the most remarkable nitrogen and phosphorus removal performance among these substrates. The average removal efficiencies of ammonia nitrogen, total nitrogen, and total phosphorus of PSM were 66.4%, 58.1%, and 85%, respectively. First-order continuous stirred-tank reactor (first-order-CSTR) and Monod continuous stirred-tank reactor (Monod-CSTR) models were established to investigate the kinetic behavior of denitrification nitrogen removal processes using different substrates. Monod-CSTR model was proven to be an accurate model that could simulate nitrate nitrogen removal performance in vertical flow constructed wetland (VFCWs). Moreover, PSM demonstrated significant pollutant removal capacity with the kinetics coefficient of 2.0021 g/m² d. Hence, PSM can be considered as a promising new type of substrate for micro-polluted wastewater treatment, and Monod-CSTR model can be employed to simulate denitrification processes.

Keywords: nitrogen; phosphorus; substrates; constructed wetland; kinetics



Citation: Zeng, Y.; Xu, W.; Wang, H.; Zhao, D.; Ding, H. Nitrogen and Phosphorus Removal Efficiency and Denitrification Kinetics of Different Substrates in Constructed Wetland. *Water* **2022**, *14*, 1757. <https://doi.org/10.3390/w14111757>

Academic Editor: Jian Liu

Received: 24 April 2022

Accepted: 23 May 2022

Published: 30 May 2022

Publisher's Note: MDPI stays neutral with regard to jurisdictional claims in published maps and institutional affiliations.



Copyright: © 2022 by the authors. Licensee MDPI, Basel, Switzerland. This article is an open access article distributed under the terms and conditions of the Creative Commons Attribution (CC BY) license (<https://creativecommons.org/licenses/by/4.0/>).

1. Introduction

Industrial wastewater, agricultural wastewater, and domestic wastewater generated in the process of human social life and production are generally treated by sewage treatment plants before discharging into rivers [1–3]. However, water from treatment plants may pollute surface water due to the limited biochemical treatment capacity and operation investment of the sewage treatment plants [4]. In addition, the combined pollution of nitrogen and phosphorus can easily lead to the eutrophication of rivers, which will further endanger the aquatic environment and human life [5,6]. Thus, advanced processes for tailwater treatment are required to ensure the safety of effluent [7]. Constructed wetlands (CWs), as an ecological water treatment technology, have the advantages of high pollutant removal efficiency, low investment and operation cost, easy management, and high landscape value and have been regarded as an efficient solution for nitrogen and phosphorus treatment of slightly polluted water [8,9].

Substrate plays an important role in CWs, and it is the key to ensure efficient nitrogen and phosphorus removal [10]. Currently, substrates can be divided into natural substrates and artificial substrates [11]. Natural substrates refer to the minerals that exist in nature, such as gravel, zeolite, manganese ore, etc., which have weak nitrogen and phosphorus removal performance. The ammonia nitrogen (NH₄⁺-N), total nitrogen (TN), and total

phosphorus (TP) removal efficiency of gravel used in CWs were 58.9%, 20.1%, and 28.8%, respectively [12]. The average removal rates of nitrogen and phosphorus of other natural substrates were less than 70% [13,14]. Artificial substrates include industrial or construction wastes [15], agricultural wastes [16], and artificially designed new substrates [17] with significant nitrogen and phosphorus removal. Li et al. [18] compared the nitrogen and phosphorus removal performance of bricks, concrete, and three natural substrates. TP removal rates of the first two artificial substrates reached 77–87%, which were better than that of natural substrates. However, the $\text{NH}_4^+\text{-N}$ and TN removal efficiencies of bricks and concrete were lower than that of zeolite by 1.6–25%. Industrial or construction wastes and agricultural wastes were rich in Ca, Mg, and C elements. Therefore, their nitrogen and phosphorus removal abilities were better than that of natural substrates [19]. However, the new substrates among artificial substrates have the most significant nitrogen and phosphorus removal performance. Bao [20] et al. synthesized iron oxide-based porous ceramsite using attapulgite, goethite, and wood chips as raw materials for treatment of domestic sewage. Compared with commercial ceramsite, the removal efficiencies of $\text{NH}_4^+\text{-N}$, TN, and TP of this new substrate were greatly improved and reached 94.2%, 46.3%, and 72.3%, respectively. The reason was that iron oxide-based porous ceramsite was rich in C, Al, Fe, and Mg elements, which are beneficial to $\text{NH}_4^+\text{-N}$ ion exchange, microbial denitrification, and phosphate precipitation.

This study constructed a laboratory-scale vertical flow constructed wetland (VFCWs) to treat slightly polluted water containing nitrogen and phosphorus. Five substrates (substrate from zeolite, bio-ceramsite, quartz sand, porous filter, and palygorskite self-assembled composite material (PSM)) were selected, and their nitrogen and phosphorus removal capacities were investigated. We also evaluated the effluent quality of micro-polluted water after substrates treatment according to the environmental quality standard for surface water in China (GB 3838-2002). Finally, two kinetics models were developed to simulate the TN treatment processes based on the above-mentioned substrates in VFCWs.

2. Materials and Methods

2.1. Substrates and Wastewater Characteristics

2.1.1. Substrate Samples

Zeolite, quartz sand, bio-ceramsite, porous filter, and PSM were employed as substrates in the established VFCWs system. Zeolite is an aluminosilicate mineral composed of silica tetrahedron and alumina tetrahedron, which is often used in wastewater treatment due to its strong adsorption, electrostatic attraction, and cation exchange properties. Quartz sand is made from natural quartz ore through crushing, water washing, and fine screening. It is widely used in water treatment industry because of its good water permeability and strong pollution interception ability. Bio-ceramsite is a lightweight material that is prepared using clay, binders, and additives. The material has high mechanical strength, stable chemical properties, easy microbial attachment and growth, and strong adsorption performance. Zeolite, quartz sand, and bio-ceramsite were purchased from Zunguan Environmental Protection Technology Co., Ltd. The porous filler employed in the present work was a hollow spherical porous filler composed of sintered clay and external porous spherical polypropylene plastic with a diameter of 5 cm. The sintered clay was a hollow spherical filler with an outer diameter of 4.5 cm and an inner diameter of 2.5 cm, which was prepared by injecting the mixture of sludge, straw, and clay into a spherical mold and then sintering at 400 °C. The palygorskite self-assembled composite material (PSM) was prepared by hydrothermal crystallization method [21] using the main raw materials of palygorskite and ferrous sulfide. The detailed preparation process of PSM was that palygorskite was calcined at 500 °C and mixed with sodium hydroxide evenly together. Then, the mixture was calcined in air at 600 °C for 2 h. The deionized water was added into the mixture and stirred vigorously for 12 h to obtain the suspension. The extracted solution containing the silica aluminum source was separated from the suspension by a filtration process. Then, an equal amount of cetyltrimethylammonium bromide and polyethylene glycol 4000 was dis-

solved into deionized water. The extracted solution was slowly added to the homogeneous solution with 1 h of stirring. After that, HNO₃ was added to adjust the pH value to 7 and continuously stirred for 2 h. Subsequently, ferrous sulfide was added to the above mixed solution and stirred for 2 h without oxygen. Finally, the mixture was transferred to an autoclave for 12 h of hydrothermal reaction without oxygen. After crystallization, the reaction product was filtered, washed repeatedly with deionized water to the pH value to 7, and dried at 80 °C without oxygen. The as-synthesized product was calcined at 400 °C without oxygen for 5 h to remove the template and form palygorskite self-assembled composite material (PSM). The physical characteristics and chemical properties of zeolite (Z), quartz sand (QS), bio-ceramsite (BC), porous filter (PF), and PSM were shown in Table 1, and all substrates were inoculated with autotrophic denitrifying bacteria.

Table 1. Physical characteristics and main chemical compositions of five substrates.

Substrates	SiO ₂ (%)	Al ₂ O ₃ (%)	Fe ₂ O ₃ (%)	MgO (%)	CaO (%)	K ₂ O (%)	Surface Area (m ² /g)	Pore Volume (cm ³ /g)	Pore Size/(nm)
Z	65.03	8.10	1.87	0.70	4.05	2.60	6.698	1.43 × 10 ⁻²	8.51
QS	50.29	7.37	6.11	1.76	8.12	4.56	4.618	2.18 × 10 ⁻⁴	468.30
BC	53.42	7.79	2.27	1.79	9.12	4.94	3.476	1.21 × 10 ⁻³	7.23
PF	59.89	10.18	3.73	2.75	10.93	2.33	7.724	1.12 × 10 ⁻³	14.67
PSM	55.15	7.31	17.38	6.34	1.52	2.11	49.23	0.93	36.50

2.1.2. Wastewater Preparation and Analysis

The experimental influent was micro-polluted wastewater prepared by NH₄Cl, KNO₃, and KH₂PO₄. The average concentrations of NH₄⁺-N and TP in synthetic wastewater prepared from NH₄Cl and KH₂PO₄ were 1.5 mg/L and 0.3 mg/L respectively, which was used to determine the NH₄⁺-N removal performance of substrates. The average concentrations of TN and TP in synthetic wastewater prepared from NH₄Cl, KNO₃, and KH₂PO₄ [c(NH₄⁺-N)/c(NO₃⁻-N) = 1:1] were 1.5 mg/L and 0.3 mg/L, respectively, which was used to determine the TN and TP removal performance of substrates. The average concentrations of NH₄⁺-N, TN, and TP in prepared synthetic wastewater all achieved water quality of Class IV water (GB 3838-2002 in China). The average concentrations of NO₃⁻-N were 1.25 mg/L, 1.50 mg/L, 1.75 mg/L, 2.00 mg/L, 2.25 mg/L, 2.50 mg/L, 2.75 mg/L, and 3.00 mg/L in synthetic wastewater prepared from KNO₃ and KH₂PO₄, which was used to determine the removal performance of substrates on NO₃⁻-N and simulate NO₃⁻-N kinetic process. The VFCWs were fed with synthetic wastewater through all the experimental period. After treatment, the effluent samples were filtered through 0.45 μm filter membranes. The contents of NH₄⁺-N, TN, and TP from influent and effluent samples were measured by Nessler's reagent colorimetric method, alkaline potassium persulfate digestion-UV spectrophotometric method, and ammonium molybdate spectrophotometric method using a UV-Vis spectrophotometer (752, Shanghai Shunyu Hengping Scientific Instrument Co., Ltd., Shanghai, China).

2.2. Wetland System and Operation

In this study, a VFCWs experimental device was constructed to compare the nitrogen and phosphorus removal efficiency of various substrates. Figure 1 illustrates the VFCWs system consisting of a storage tank with synthetic wastewater, a peristaltic pump, a VFCWs unit, and an effluent tank. The VFCWs unit was a vertical PVC column with a diameter of 10 cm and a height of 100 cm, which was filled with the selected substrates.

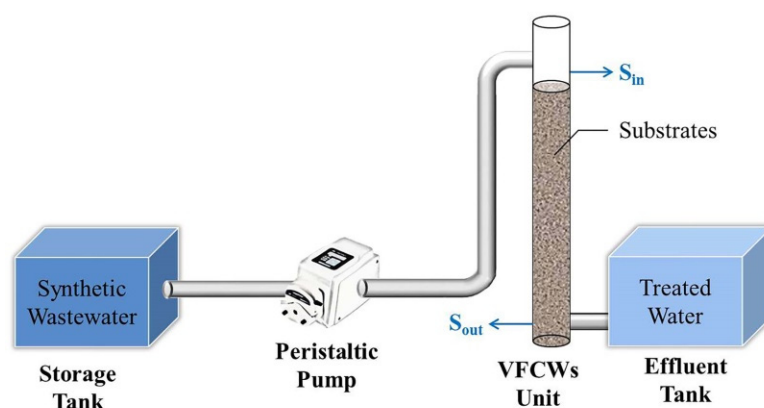


Figure 1. Schematic diagram of VFCWs experimental device.

In the operation process, we first injected the synthetic wastewater into the top of the PVC column through a peristaltic pump. Then, the wastewater flowed through the substrate bed and reached the bottom of the PVC column and finally flowed into the effluent tank. In this experiment, the mode of operation in the VFCWs experiment was tidal flow, the hydraulic load was $0.25 \text{ m}^3/\text{m}^2 \text{ d}$, the duration of each cycle was 30 days, and it ran 8 h every day. At the beginning of wetland system operation, all sampling ports (S_{in} and S_{out} in Figure 1) of the PVC column should be closed. The influent flow was adjusted by a flow meter. After 8 h of operation, water samples were collected from the water outlet (S_{out} in Figure 1) of VFCWs unit and then detected. The water inlet and outlet were closed at the end of the experiment on first day. When the system was operated for another day, the water inlet and outlet were opened directly. After 8 h of operation, water samples were collected from the water outlet (S_{out} in Figure 1) of VFCWs unit and then detected. After one cycle, the water in the wetland system was emptied for the next experimental cycles.

2.3. Kinetics Modeling

Two kinetic models were developed in this section to simulate the process of removing nitrate nitrogen in VFCWs. Approach 1: assuming that the pollutant reduction process conformed to the simplified first-order-CSTR model; Approach 2: assuming that the pollutant reduction process conformed to the simplified Monod-CSTR model. The reason for combining kinetics with CSTR flow pattern was that synthetic wastewater in VFCWs filled with substrates would flow in all directions of the main flow direction, which conformed to the CSTR flow pattern rather than the plug flow pattern. The simplified first-order-CSTR model and simplified Monod-CSTR model were suitable for wetland systems containing substrates under intermittent inflow mode. Since the constructed wetland system was packed with substrates and batch fed (in flushes) with wastewater, the local flow direction of the wastewater at any random position was likely to diverge rapidly (by the saturated and unsaturated substrates) from the bulk flow direction during downwards flow, resembling CSTR flow pattern [22–24].

First-order kinetic model is described as follows:

$$\frac{dC}{dt} = -k_v C_{out} \quad (1)$$

where $\frac{dC}{dt}$ represents concentration at time t ($\text{mg}/\text{L d}$), k_v represents volumetric rate constant (d^{-1}), and C_{out} represents outlet pollutant concentration (mg/L).

The Monod kinetic model is described as follows:

$$\frac{dC}{dt} = -K_{max} \frac{C_{out}}{C_{half} + C_{out}} \quad (2)$$

where K_{\max} represents maximum volumetric pollutant removal rates ($\text{g}/\text{m}^3 \text{ d}$); C_{half} represents half saturation constant of limiting substrate (mg/L).

CSTR flow pattern in a reactor is described as follows:

$$\frac{dC}{dt} + \frac{1}{\tau}C_{\text{in}} = \frac{1}{\tau}C_{\text{out}} \quad (3)$$

where τ represents hydraulic retention time (d); C_{in} represents inlet pollutant concentration (mg/L).

Combining Equations (1) and (3) resulted a simplified first-order-CSRT model as expressed in Equation (4). Combining Equations (2) and (3) resulted in a simplified Monod-CSRT model as expressed in Equation (5).

$$q(C_{\text{in}} - C_{\text{out}}) = K_1 C_{\text{out}} \quad (4)$$

$$q(C_{\text{in}} - C_{\text{out}})(C_{\text{half}} + C_{\text{out}}) = K_2 C_{\text{out}} \quad (5)$$

where q represents hydraulic loading ($\text{m}^3/\text{m}^2 \text{ d}$), K_1 represents areal rate constant (m/d), K_2 represents maximum areal pollutant removal rate ($\text{g}/\text{m}^2 \text{ d}$), and C_{half} for $\text{NO}_3^- - \text{N}$ was $0.14 \text{ mg}/\text{L}$ in Monod-CSRT model [25].

Coefficient of determination (R^2), relative root mean square error (RRMSE), and model efficiency (ME) were used to investigate the relationship between the predicted value of the model and the experimental value. The present work compared the applicability of first-order-CSRT model and Monod-CSRT model by analyzing these three statistical indexes. R^2 ranged from 0 to 1, and experimental data fitted better as R^2 was close to 1. The range of RRMSE was $0 \sim \infty$. Low RRMSE illustrated that the predicted value was close to the experimental value. The range of ME was $-\infty$ to 1, and the model could be applied to describe the experimental results when ME was close to 1. The calculation formula of R^2 , RRMSE, and ME were as follows:

$$R^2 = \frac{|\sum_{i=1}^N (x_i - \bar{x})(y_i - \bar{y})|^2}{\sum_{i=1}^N (x_i - \bar{x})^2 \sum_{i=1}^N (y_i - \bar{y})^2} \quad (6)$$

$$\text{RRMSE} = \frac{\sqrt{(1/N) \sum_{i=1}^N (y_i - \hat{y})^2}}{\bar{y}} \quad (7)$$

$$\text{ME} = 1 - \frac{\sum_{i=1}^N (y_i - \hat{y})^2}{\sum_{i=1}^N (y_i - \bar{y})^2} \quad (8)$$

where x_i and y_i are two sets of data, \bar{x} and \bar{y} are mean of the data, y_i is experimental results, and \hat{y}_i is predictive value.

3. Results and Discussion

3.1. Ammonia Nitrogen Removal Efficiencies of the Substrates

It could be seen from Figure 2a that the $\text{NH}_4^+ - \text{N}$ treatment capacities of zeolite (Z), quartz sand (QS), bio-ceramsite (BC), porous filler (PF), and PSM within 30 days gradually decreased with the increase of time. The $\text{NH}_4^+ - \text{N}$ removal efficiencies of zeolite, porous filler, and PSM showed a similar trend of rapidly decline at first and then stabilizing. The results of the three substrates indicated that adsorption rates of substrates were faster in the early stage and then became stable when the dynamic equilibrium of adsorption-desorption was achieved. The three substrates presented good $\text{NH}_4^+ - \text{N}$ treatment efficiencies, and the highest removal rate could reach more than 90%. However, the highest removal rates of quartz sand and bio-ceramsite were only 56% and 65%, respectively. The order of treatment performance of five substrates was PSM > zeolite > porous filler > quartz sand > bio-ceramsite, while their average removal rates were 66.4%, 64%, 61%, 41.7%, and 33.3%, respectively. Figure 2b described that the $\text{NH}_4^+ - \text{N}$ concentrations in a water body

treated by the substrates were greatly reduced. In particular, the quality of effluent treated with PSM, zeolite, and porous filler was improved from Class IV water to Class III water (≤ 1 mg/L) and could meet Class III water standard within 30 days. The reasons for better ammonia nitrogen removal efficiencies of PSM, zeolite, and porous filler were: (1) The three substrates had larger specific surface area and pore volume, which improved the electrostatic attraction and physical adsorption capacities of substrates [26], and (2) the three substrates were rich in Si, Al, and K elements, which enhanced the ion exchange between substrates and $\text{NH}_4^+\text{-N}$ [27].

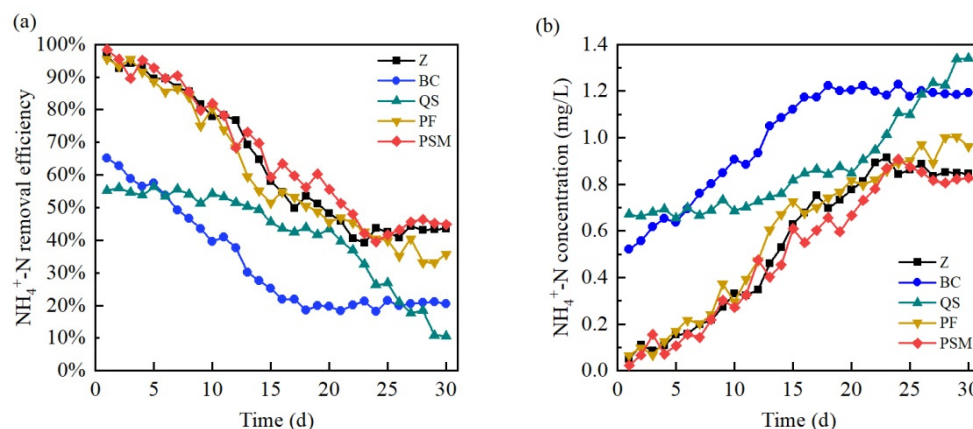


Figure 2. $\text{NH}_4^+\text{-N}$ removal efficiencies of five substrates: (a) $\text{NH}_4^+\text{-N}$ removal efficiency; (b) $\text{NH}_4^+\text{-N}$ concentration of effluent.

3.2. Total Nitrogen Removal Efficiencies of the Substrates

Figure 3a illustrated the TN removal efficiencies of all substrates gradually decreased. While PSM, porous filler, and zeolite showed high ammonia nitrogen removal efficiencies, the three substrates also possessed good TN treatment performance, and the average removal efficiency reached 49.1–58.1%. However, the removal rates of quartz sand and bio-ceramsite were only 33.1% and 16.6%, respectively. The TN removal order of substrates was PSM > porous filler > zeolite > quartz sand > bio-ceramsite. Further, the TN removal capacities of selected substrates were lower than $\text{NH}_4^+\text{-N}$ removal rates, indicating that the denitrification ability of microorganisms on these substrates was weaker than the adsorption ability of substrates. The reason was that adaptability of microorganisms attached to substrates was weak at the initial stage, and the reproduction rate of microorganisms was less than their extinction rate, and subsequently, microorganisms adapting to this environment grew stably. According to Figure 3b, the TN content in effluent treated by substrates could meet the standard for Class IV water (≤ 1.5 mg/L) within 30 days. Specially, after the treatment using PSM, porous filler, and zeolite, the effluent quality all reached Class III water standard (≤ 1 mg/L). PSM had better denitrification efficiency than porous fillers and zeolite. The reason for this result is that electron-donor-providing PSM cooperated with microorganisms to convert nitrate nitrogen into nitrogen gas without addition of carbon sources and promoted TN removal. In addition, high specific surface area and large pore volume of PSM facilitated adhesion and growth of microorganisms, which further promoted denitrification reaction [28]. Consequently, PSM has a great potential for TN removal in VFCWs.

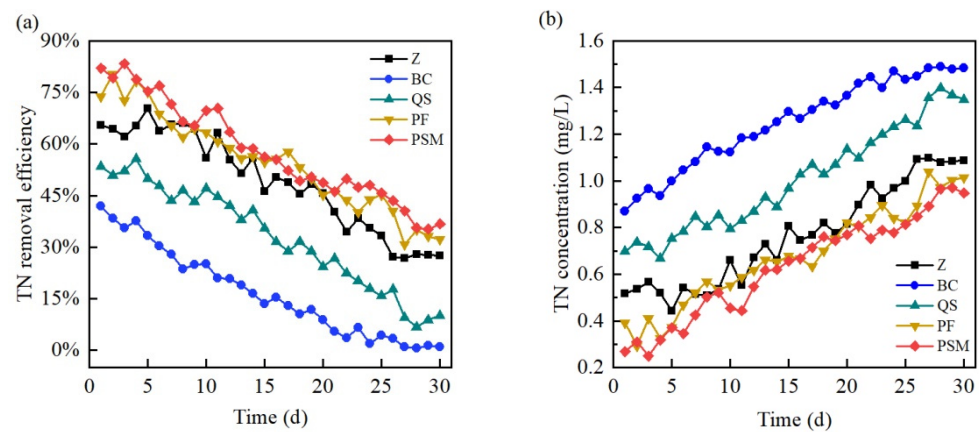


Figure 3. TN removal efficiencies of five substrates: (a) TN removal efficiency; (b) TN concentration of effluent.

3.3. Total Phosphorus Removal Efficiencies of the Substrates

Figure 4 exhibited TP removal efficiencies of five substrates, and the order of treatment performance was PSM > bio-ceramsite > porous filler > quartz sand > zeolite. TP removal efficiencies of PSM decreased first and then increased. The reason was that the reaction capability of substrates, microorganisms, and nitrate nitrogen was weak in the early stage, and released iron ions and aluminum ions were gradually decreased, resulting in the weakening of the chemical reaction between metal ions and phosphate. With stable reproduction of microorganisms, the metal ions were released from substrates into water. Then, the complexation between metal ions and phosphate was promoted, which restored the TP removal capacity of PSM with the average removal efficiency of 85%. TP removal efficiencies of porous filler, zeolite, bio-ceramsite, and quartz sand dropped sharply within 20 days. After 10 to 15 days, TP removal rates of various substrates were lower than 0%. The effluent TP concentration rose to 0.3 mg/L, even higher than the original level, because the phosphorus adsorbed by the substrates was partially desorbed and released back into the water after these substrates reached adsorption equilibrium. Hence, PSM was proven to be the best substrate for TP removal among the selected materials, which increased the water quality from Class IV (0.3 mg/L) to Class III (0.2 mg/L) and stabilized for 30 days. The main reasons for the remarkable performance of PSM were as follows: (1) The iron ions and aluminum ions generated by substrates and microorganisms in the nitrate nitrogen removal process would enhance complexation of metal ions and phosphate; (2) PSM itself was rich in Fe and Mg elements, which was conducive to the complexation reaction between metal ions and phosphate [29].

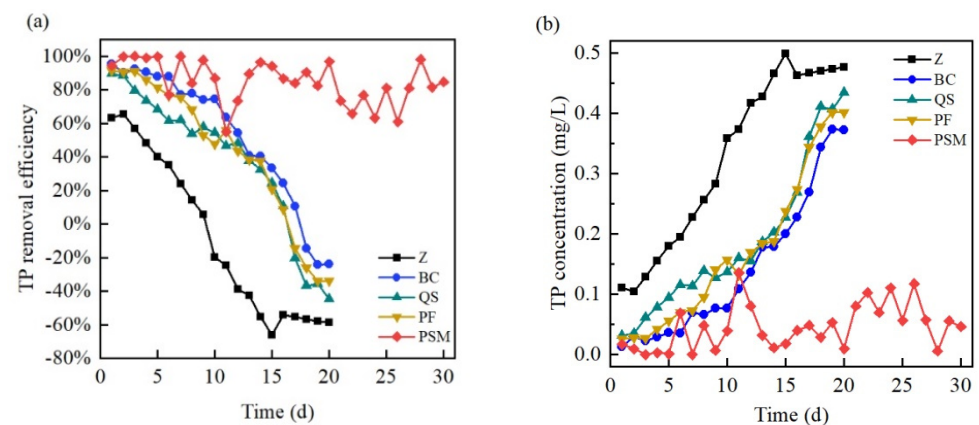


Figure 4. TP removal efficiencies of five substrates: (a) TP removal efficiency; (b) TP concentration of effluent.

3.4. Dynamic Simulation and Kinetics Analysis

In this section, simplified first-order-CSTR and Monod-CSTR models were used to simulate the nitrate nitrogen removal processes based on zeolite, quartz sand, bio-ceramsite, porous filler, and PSM. In Figures 5–9, the R^2 values ($R^2 = ME$) of Monod-CSTR model are higher than that of first-order-CSTR model for the substrates. Meanwhile, the RRMSE values of Monod-CSTR model were also lower, which illustrated that Monod-CSTR model was more suitable for simulating and predicting the NO_3^- -N removal processes. The simulated rate coefficients (K_2) of zeolite, quartz sand, bio-ceramsite, porous filler, and PSM in the Monod-CSTR model were 0.7643 $\text{g}/\text{m}^2 \text{d}$, 0.6392 $\text{g}/\text{m}^2 \text{d}$, 0.3191 $\text{g}/\text{m}^2 \text{d}$, 0.9717 $\text{g}/\text{m}^2 \text{d}$, and 2.0021 $\text{g}/\text{m}^2 \text{d}$, respectively. The results showed that the order of the substrates in terms of the efficiency of contamination removal was consistent with the experimental results: PSM > porous filler > zeolite > quartz sand > bio-ceramsite. The experimental results are shown in Table 2. The order of R^2 value of five substrates in the Monod-CSTR model was porous filler > PSM > zeolite > bio-ceramsite > quartz sand. Monod-CSTR model was successfully applied to simulate the NO_3^- -N removal processes that employed porous filler, PSM, and zeolite as substrates since the R^2 values of the three substrates were higher than 0.95. Based on the kinetics studies, the Monod-CSTR model could be used to simulate and predict the denitrification process of PSM in VECWs.

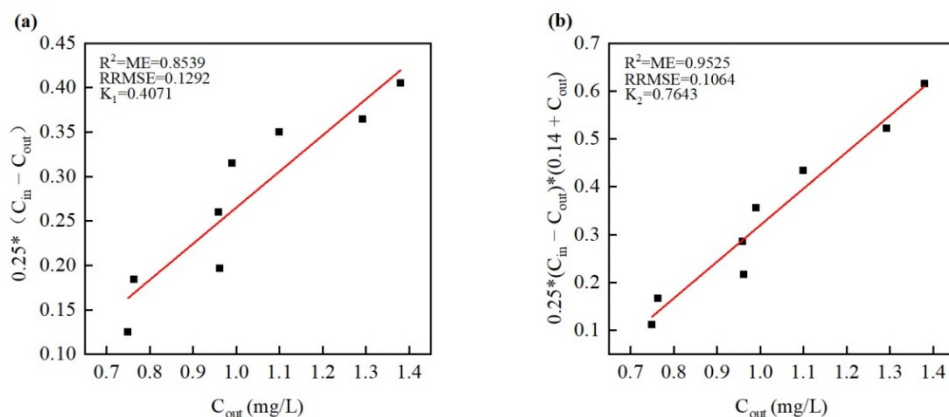


Figure 5. Regression of kinetics models for NO_3^- -N removal by zeolite: (a) first-order-CSTR model; (b) Monod-CSTR model.

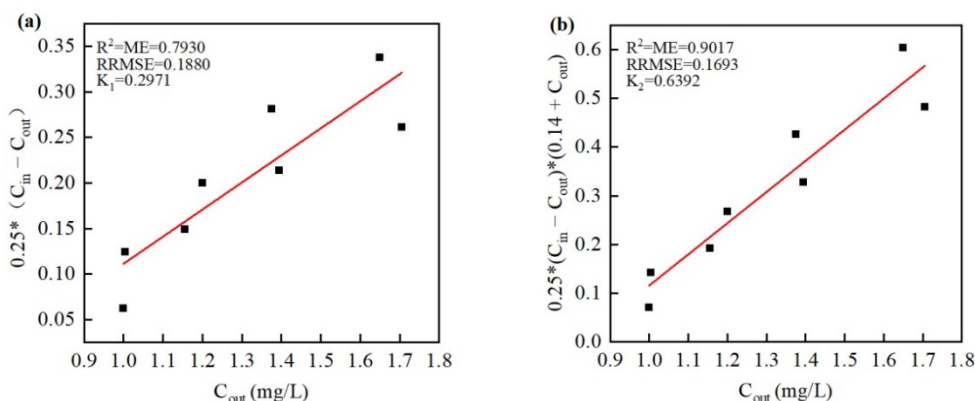


Figure 6. Regression of kinetics models for NO_3^- -N removal by quartz sand: (a) first-order-CSTR model; (b) Monod-CSTR model.

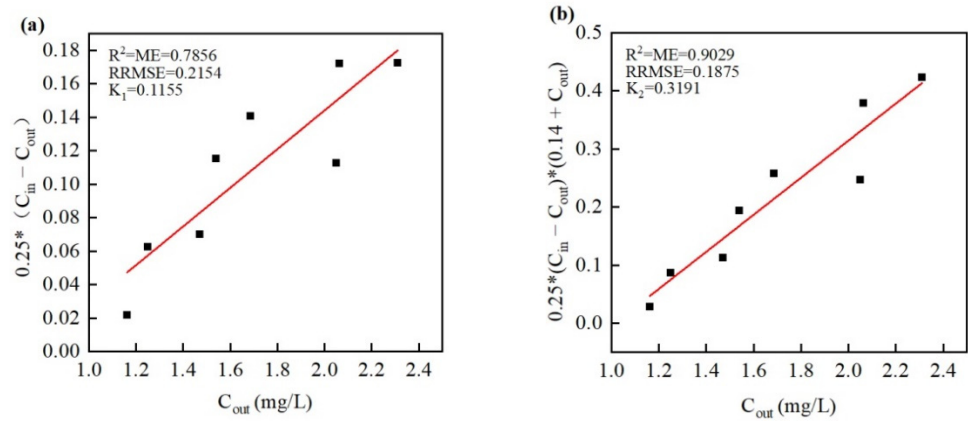


Figure 7. Regression of kinetics models for NO₃⁻-N removal by bio-ceramsite: (a) first-order-CSTR model; (b) Monod-CSTR model.

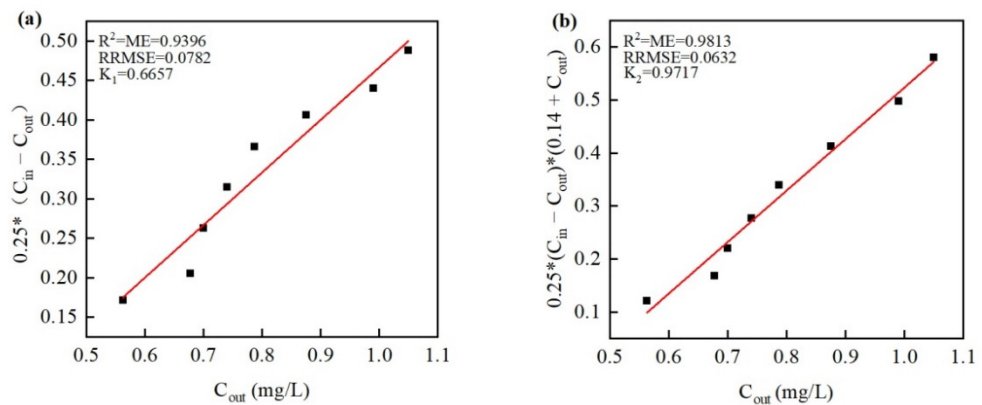


Figure 8. Regression of kinetics models for NO₃⁻-N removal by porous filler: (a) first-order-CSTR model; (b) Monod-CSTR model.

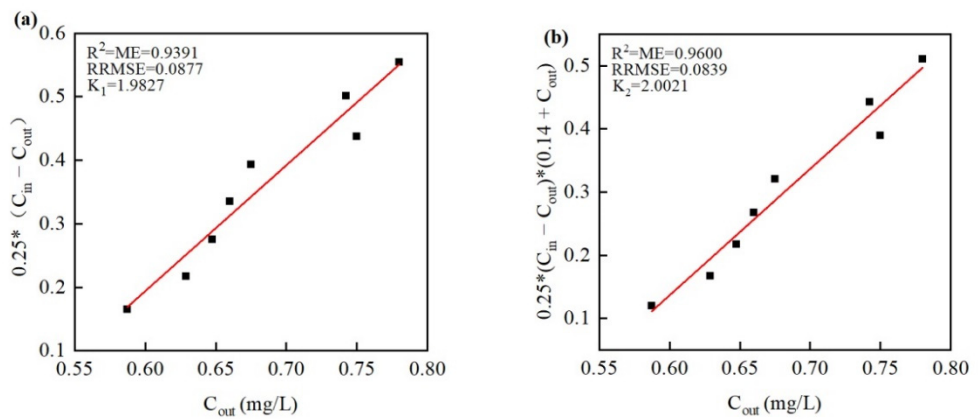


Figure 9. Regression of kinetics models for NO₃⁻-N removal by PSM: (a) first-order-CSTR model; (b) Monod-CSTR model.

Table 2. Kinetic experimental data of five substrates for denitrification.

C_{in}	Zeolite		Quartz Sand		Bio-Ceramsite		Porous Filter		PSM	
	C_{out} (mg/L)	Removal Rate (%)								
1.25	0.75	40.00	1.00	20.00	1.16	7.20	0.56	55.20	0.59	52.80
1.50	0.76	49.33	1.00	33.33	1.25	16.67	0.68	54.67	0.63	58.00
1.75	0.96	45.14	1.16	33.71	1.47	16.00	0.70	60.00	0.65	62.86
2.00	0.96	52.00	1.20	40.00	1.54	23.00	0.74	63.00	0.66	67.00
2.25	0.99	56.00	1.40	37.78	1.69	24.89	0.79	64.89	0.68	69.78
2.50	1.10	56.00	1.38	44.80	2.05	18.00	0.88	64.80	0.76	69.60
2.75	1.29	53.09	1.71	37.82	2.06	25.09	0.99	64.00	0.74	73.09
3.00	1.38	54.00	1.65	45.00	2.31	23.00	1.05	65.00	0.78	74.00

4. Conclusions

Compared with the natural substrates (zeolite and quartz sand) and the existing substrate (bio-ceramsite and porous filler), the new type of substrate (palygorskite self-assembled composite material (PSM)) prepared in this paper displayed more remarkable nitrogen and phosphorus removal performance. PSM was proved to be the best substrate among the selected materials, with the highest $\text{NH}_4^+\text{-N}$, TN, and TP removal efficiency. For other substrates, zeolite and porous fillers also showed good removal performance for $\text{NH}_4^+\text{-N}$ and TN, while the effluent quality also satisfied Class III water in China (GB 3838-2002) within 30 days. Bio-ceramsite and porous fillers had high TP removal rates at the beginning of the process, but their capacities for removing TP significantly dropped after 18 days. Therefore, PSM with efficient and significant nitrogen and phosphorus removal performance shows a possible potential for use in constructed wetlands. The first-order-CSTR model and Monod-CSTR model were developed to describe the $\text{NO}_3^-\text{-N}$ removal kinetics of the substrates. The prediction results using Monod-CSTR model matched actual experimental results. The simulated kinetic coefficient for PSM was higher than that of other substrates in Monod-CSTR model. The order of the substrates in terms of the efficiency of contamination removal was PSM > porous filler > zeolite > quartz sand > bio-ceramsite. Thus, the Monod-CSTR model was proven to be a suitable model for prediction of denitrification process in VFCWs.

Author Contributions: Conceptualization, W.X. and Y.Z.; methodology, Y.Z. and D.Z.; formal analysis, W.X.; investigation, Y.Z.; resources, W.X. and H.D.; data curation, H.W.; writing—original draft preparation, H.W. and D.Z.; writing—review and editing, W.X., D.Z. and H.D.; visualization, H.W.; supervision, D.Z. and H.D.; project administration, W.X.; funding acquisition, Y.Z. All authors have read and agreed to the published version of the manuscript.

Funding: This research was funded by “2019 science and technology project of Huadong Engineering (Fujian) Corporation”, grant number FH2019-KY002; “Key Research and Development Plan of Tianjin”, grant number 20YFZCSN00430.

Institutional Review Board Statement: Not applicable.

Informed Consent Statement: Not applicable.

Data Availability Statement: The authors confirm that the data supporting the findings of this study are available within the article. Raw data that support the findings of this study are available from the corresponding authors, upon reasonable request.

Acknowledgments: Thanks are given to Rui Zhao for her work in data collection.

Conflicts of Interest: The authors declare no conflict of interest.

References

1. Saeed, T.; Muntaha, S.; Rashid, M.; Sun, G.; Hasnat, A. Industrial wastewater treatment in constructed wetlands packed with construction materials and agricultural by-products. *J. Clean. Prod.* **2018**, *189*, 442–453. [[CrossRef](#)]
2. Kilingo, F.M.; Bernard, Z.; Hongbin, C. Study of domestic wastewater treatment using *Moringa oleifera* coagulant coupled with vertical flow constructed wetland in Kibera Slum, Kenya. *Environ. Sci. Pollut. Res.* **2022**, *29*, 36589–36607. [[CrossRef](#)] [[PubMed](#)]
3. Li, J.; Zheng, B.; Chen, X.; Li, Z.; Xia, Q.; Wang, H.; Yang, Y.; Zhou, Y.; Yang, H. The use of constructed wetland for mitigating nitrogen and phosphorus from agricultural runoff: A Review. *Water* **2021**, *13*, 476. [[CrossRef](#)]
4. Zheng, F.; Fang, J.; Guo, F.; Yang, X.; Liu, T.; Chen, M.; Nie, M.; Chen, Y. Biochar based constructed wetland for secondary effluent treatment: Waste resource utilization. *Chem. Eng. J.* **2022**, *432*, 134377. [[CrossRef](#)]
5. Cheng, R.; Zhu, H.; Shutes, B.; Yan, B. Treatment of microcystin (MC-LR) and nutrients in eutrophic water by constructed wetlands: Performance and microbial community. *Chemosphere* **2021**, *263*, 128139. [[CrossRef](#)]
6. Shen, S.; Geng, Z.; Li, X.; Lu, X. Evaluation of phosphorus removal in floating treatment wetlands: New insights in non-reactive phosphorus. *Sci. Total Environ.* **2022**, *815*, 152896. [[CrossRef](#)]
7. Ni, Q.; Wang, T.; Liao, J.; Shi, W.; Huang, Z.; Miao, H.; Wu, P.; Ruan, W. Operational performances and enzymatic activities for eutrophic water treatment by vertical-flow and horizontal-flow constructed wetlands. *Water* **2020**, *12*, 2007. [[CrossRef](#)]
8. Khalifa, M.E.; El-Reash, Y.G.A.; Ahmed, M.I.; Rizk, F.W. Effect of media variation on the removal efficiency of pollutants from domestic wastewater in constructed wetland systems. *Ecol. Eng.* **2020**, *143*, 105668. [[CrossRef](#)]
9. Maharjan, A.K.; Mori, K.; Toyama, T. Nitrogen removal ability and characteristics of the laboratory-scale tidal flow constructed wetlands for treating ammonium-nitrogen contaminated groundwater. *Water* **2020**, *12*, 1326. [[CrossRef](#)]
10. Ji, Z.; Tang, W.; Pei, Y. Constructed wetland substrates: A review on development, function mechanisms, and application in contaminants removal. *Chemosphere* **2022**, *286*, 131564. [[CrossRef](#)]
11. Wang, Y.; Cai, Z.; Sheng, S.; Pan, F.; Chen, F.; Fu, J. Comprehensive evaluation of substrate materials for contaminants removal in constructed wetlands. *Sci. Total Environ.* **2020**, *701*, 134736. [[CrossRef](#)] [[PubMed](#)]
12. Saeed, T.; Miah, M.J.; Majed, N.; Hasan, M.; Khan, T. Pollutant removal from landfill leachate employing two-stage constructed wetland mesocosms: Co-treatment with municipal sewage. *Environ. Sci. Pollut. Res.* **2020**, *27*, 28316–28332. [[CrossRef](#)] [[PubMed](#)]
13. Li, Y.; Bai, X.; Ding, R.; Lv, W.; Long, Y.; Wei, L.; Xiang, F.; Wang, R. Removal of phosphorus and ammonium from municipal wastewater treatment plant effluent by manganese ore in a simulated constructed wetland. *Environ. Sci. Pollut. Res.* **2021**, *28*, 41169–41180. [[CrossRef](#)] [[PubMed](#)]
14. Ge, Z.; Wei, D.; Zhang, J.; Hu, J.; Liu, Z.; Li, R. Natural pyrite to enhance simultaneous long-term nitrogen and phosphorus removal in constructed wetland: Three years of pilot study. *Water Res.* **2019**, *148*, 153–161. [[CrossRef](#)] [[PubMed](#)]
15. Xu, R.; Zhang, Y.; Liu, R.; Cao, Y.; Wang, G.; Ji, L.; Xu, Y. Effects of different substrates on nitrogen and phosphorus removal in horizontal subsurface flow constructed wetlands. *Environ. Sci. Pollut. Res.* **2019**, *26*, 16229–16238. [[CrossRef](#)]
16. Wang, R.; Zhao, X.; Liu, H.; Wu, H. Elucidating the impact of influent pollutant loadings on pollutants removal in agricultural waste-based constructed wetlands treating low C/N wastewater. *Bioresour. Technol.* **2019**, *273*, 529–537. [[CrossRef](#)]
17. Wang, H.; Xu, J.; Liu, Y.; Sheng, L. Preparation of ceramsite from municipal sludge and its application in water treatment: A review. *J. Environ. Manag.* **2021**, *287*, 112374. [[CrossRef](#)]
18. Li, H.; Zhang, Y.; Wu, L.; Jin, Y.; Gong, Y.; Li, A.; Li, J.; Li, F. Recycled aggregates from construction and demolition waste as wetland substrates for pollutant removal. *J. Clean. Prod.* **2021**, *311*, 127766. [[CrossRef](#)]
19. Saeed, T.; Miah, M.J.; Khan, T.; Ove, A. Pollutant removal employing tidal flow constructed wetlands: Media and feeding strategies. *Chem. Eng. J.* **2020**, *382*, 122874. [[CrossRef](#)]
20. Bao, T.; Chen, T.; Tan, J.; Wille, M.; Zhu, D.; Chen, D.; Xi, Y. Synthesis and performance of iron oxide-based porous ceramsite in a biological aerated filter for the simultaneous removal of nitrogen and phosphorus from domestic wastewater. *Sep. Purif. Technol.* **2016**, *167*, 154–162. [[CrossRef](#)]
21. Guan, Y.; Wang, S.; Wang, X.; Sun, C.; Huang, Y.; Liu, C.; Zhao, H. In situ self-assembled synthesis of Ag-AgBr/Al-MCM-41 with excellent activities of adsorption-photocatalysis. *Appl. Catal. B-Environ.* **2017**, *209*, 329–338. [[CrossRef](#)]
22. Weerakoon, G.M.P.R.; Jinadasa, K.B.S.N.; Manatunge, J.; Wijesiri, B.; Goonetilleke, A. Kinetic modelling and performance evaluation of vertical subsurface flow constructed wetlands in tropics. *J. Water Process. Eng.* **2020**, *38*, 101539. [[CrossRef](#)]
23. Saeed, T.; Sun, G.Z. Kinetic modelling of nitrogen and organics removal in vertical and horizontal flow wetlands. *Water Res.* **2011**, *45*, 3137–3152. [[CrossRef](#)] [[PubMed](#)]
24. Saeed, T.; Sun, G.Z. The removal of nitrogen and organics in vertical flow wetland reactors: Predictive models. *Bioresour. Technol.* **2011**, *102*, 1205–1213. [[CrossRef](#)] [[PubMed](#)]
25. Saeed, T.; Miah, M.J.; Khan, T. Intensified constructed wetlands for the treatment of municipal wastewater: Experimental investigation and kinetic modelling. *Environ. Sci. Pollut. Res.* **2021**, *28*, 30908–30928. [[CrossRef](#)] [[PubMed](#)]
26. Zhao, J.; Zhao, Y.; Xu, Z.; Doherty, L.; Liu, R. Highway runoff treatment by hybrid adsorptive media-baffled subsurface flow constructed wetland. *Ecol. Eng.* **2016**, *91*, 231–239. [[CrossRef](#)]
27. Tan, X.; Yang, Y.; Liu, Y.; Li, X.; Fan, X.; Zhou, Z.; Liu, C.; Yin, W. Enhanced simultaneous organics and nutrients removal in tidal flow constructed wetland using activated alumina as substrate treating domestic wastewater. *Bioresour. Technol.* **2019**, *280*, 441–446. [[CrossRef](#)]

28. Shen, S.; Li, X.; Cheng, F.; Zha, X.; Lu, X. Review: Recent developments of substrates for nitrogen and phosphorus removal in CWs treating municipal wastewater. *Environ. Sci. Pollut. Res.* **2020**, *27*, 29837–29855. [[CrossRef](#)]
29. Cheng, S.; Qin, C.; Xie, H.; Wang, W.; Zhang, J.; Hu, Z.; Liang, S. Comprehensive evaluation of manganese oxides and iron oxides as metal substrate materials for constructed wetlands from the perspective of water quality and greenhouse effect. *Ecotox. Environ. Saf.* **2021**, *221*, 112451. [[CrossRef](#)]